

**D**ouglas Swanson is a senior physics major at Yale University. In addition to plasma physics, he has conducted research in experimental nuclear physics and cosmology, and is a member of the nuclear structure group at Yale's Wright Nuclear Structure Laboratory. He is a 2007 National Science Foundation Graduate Research Fellow.

**J**onathan Menard is Principal Research Physicist and lecturer at the Princeton Plasma Physics Laboratory (PPPL). He is an experimental plasma physicist

who works primarily on the National Spherical Torus Experiment (NSTX) at PPPL. Dr. Menard's research interests include the linear and non-linear magnetohydrodynamic (MHD) stability properties of spherical torus (ST) plasmas, advanced operating scenarios in the ST, plasma startup, and wave physics. Among his honors, Dr. Menard received the Presidential Early Career Award for Scientists and Engineers in 2004, and was a recipient of the Kaul Prize in 2006.

## CALCULATION OF PARTICLE BOUNCE AND TRANSIT TIMES ON GENERAL GEOMETRY FLUX SURFACES

DOUGLAS SWANSON AND JONATHAN MENARD

### ABSTRACT

A viable nuclear fusion reactor must confine energetic plasmas long enough so that the fusion energy produced exceeds the energy consumed to heat the plasma and maintain confinement. It is well-known that magnetohydrodynamic (MHD) or plasma fluid instabilities limit confinement. One such important instability is the resistive wall mode (RWM). Plasma rotation faster than a critical frequency has been observed to stabilize the RWM. Some theories predict that the critical frequency will vary inversely with the characteristic times particles take to orbit the plasma. Previous calculations of these orbit times have assumed high aspect ratio and circular plasma cross-section, approximations unsuitable for the National Spherical Torus Experiment (NSTX). Analytic solutions for the orbit times have been derived as functions of particle energy and magnetic moment for low aspect ratio and elliptical cross-sections. Numeric solutions for arbitrary aspect ratio and cross-sectional geometry were also computed using Mathematica and IDL and agree with the analytic forms. In typical parameter regimes for NSTX, the generalized orbit times can differ from the high aspect ratio, circular approximations by as much as 40%. This result might help to assess how accurately theory describes RWM stabilization in NSTX. If theory and experiment are found to agree, generalized orbit times can be used to predict RWM stabilization in low aspect ratio nuclear fusion reactors.

### INTRODUCTION

In a nuclear fusion reactor, energy is released when plasma particles fuse. A viable reactor must confine energetic plasmas long enough so that the fusion energy produced exceeds the energy consumed to heat the plasma and maintain confinement. It is well-known that magnetohydrodynamic (MHD) or plasma fluid instabilities limit confinement. Instabilities arise from current or pressure gradients in the plasma, and result in turbulence and energy loss [1]. To maximize the efficiency and fusion power output from a toroidal fusion reactor (tokamak), it is essential to control MHD instabilities.

One such important instability is the resistive wall mode (RWM), which grows due to electrical resistivity in the walls surrounding the plasma [2]. Plasma rotation faster than a critical frequency has been observed to stabilize the RWM [3]. Some theories, including the kinetic damping theory of Bondeson and Chu, predict that the critical frequency will vary inversely with the characteristic times particles take to orbit the plasma [4]. These orbit times fall into two categories. Transit times are orbit times for particles with small magnetic moments that complete full orbits around the plasma. Bounce times are orbit times for particles with large magnetic moments that are trapped by the magnetic mirror effect and cannot complete full orbits around the plasma.

Previous calculations of these bounce and transit times have assumed high aspect ratio and circular plasma cross-section, approximations unsuitable for the National Spherical Torus Experiment (NSTX). NSTX maintains aspect ratios,  $A$ , of around 1.3 to 1.6, whereas previous calculations were for aspect ratios of 2.5 and above. NSTX also routinely achieves elongations (ellipticities)  $\kappa$  of 1.8 to 3, as compared with a purely circular cross-section ( $\kappa=1$ ).

Experimentally-measured critical rotation frequencies in the DIII-D tokamak can differ by a factor of 2 from previously predicted values [5]. Although such comparisons have not been made for NSTX, a similar disparity is predicted. Since the critical rotation frequency depends strongly on bounce and transit times, it is hypothesized that generalizing these times to NSTX parameter regimes might improve predictions of critical frequencies and RWM stabilization; important for maximizing the efficiency of a spherical torus (low aspect ratio) fusion reactor. This also might test how accurately Bondeson and Chu's kinetic damping theory describes RWM stabilization in NSTX. Hence it is desirable to calculate bounce and transit times for arbitrary aspect ratios and cross-sections (flux surface geometry).

This paper will consider analytic and numeric solutions for bounce and transit times in the general geometry case.

## MATERIALS AND METHODS

### Analytic Solutions

Analytic solutions for bounce and transit times  $\tau$  may be derived as functions of particle energy  $E$  and magnetic moment  $\mu$  for arbitrary aspect ratio and flux surface geometry. Bounce and transit times are defined by:

$$\tau = \oint \frac{ds}{v_{\parallel}} \quad (1)$$

where  $v_{\parallel}$  is the component of particle velocity parallel to the magnetic field and  $ds$  is a differential of arc length along the magnetic field lines. For transit times  $\tau_t$  the integral is taken along the magnetic field lines over a full cross-sectional circuit. For bounce times  $\tau_b$  it is taken between adjacent bounce points.

Using conservation of energy and the adiabatic invariance of the magnetic moment, the parallel velocity  $v_{\parallel}$  may be written as:

$$v_{\parallel} = \sqrt{\frac{2}{m} (E - \mu B)} \quad (2)$$

where  $B$  is the magnitude of the magnetic field at every point in space and  $m$  is the particle mass. Then the bounce and transit times become:

$$\tau = \sqrt{\frac{m}{2}} \oint \frac{ds}{\sqrt{E - \mu B}} \quad (3)$$

For trapped particles, bounce points occur where  $E = \mu B$ . The problem of calculating bounce and transit times requires evaluating this integral for any  $B$  and  $ds$ .

Figure 1 illustrates the coordinates and parameters used in the derivations below. Two different coordinate systems will be employed: an  $(r, \theta, \phi)$  toroidal coordinate system and an  $(R, Z, \phi)$  cylindrical coordinate system. The aspect ratio  $A$  is defined as  $A = R_0 / a$ .

In the high aspect ratio, circular flux surface limit considered previously,  $B$  may be taken to vary as  $1/R$ , where  $R = R_0 + r \cos \theta$  is the standard cylindrical radial coordinate. This may be expanded to first order in the small parameter  $\epsilon = r/R_0 \ll 1$  to yield  $B \approx B_0(1 - \epsilon \cos \theta)$ , with  $B_0 = B(R = R_0)$ . The same first order approximation gives  $ds \approx (R_0 q) d\theta$ , where the safety factor  $q$  represents the number of toroidal transits made by the magnetic field lines per poloidal transit. The integral above may then be evaluated analytically to obtain:

$$\tau \approx \sqrt{\frac{m}{2}} \oint \frac{R_0 q}{\sqrt{E - \mu B_0 (1 - \epsilon \cos \theta)}} d\theta$$

$$= q R_0 \sqrt{\frac{2m}{E - \mu B_0 (1 - \epsilon)}} F\left(\frac{\theta}{2} \middle| \frac{2\mu B_0 \epsilon}{E - \mu B_0 (1 - \epsilon)}\right) \quad (4)$$

where  $F$  is the incomplete elliptic integral of the first kind. This result is due to Bondeson and Chu [4].

For the arbitrary aspect ratio and flux surface cases, the above approximations for  $B$  and  $ds$  must be generalized. Consider a generic equilibrium where the poloidal flux  $\Psi$  is given in terms of the radial coordinate  $r$  and minor radius  $a$  of the plasma by:

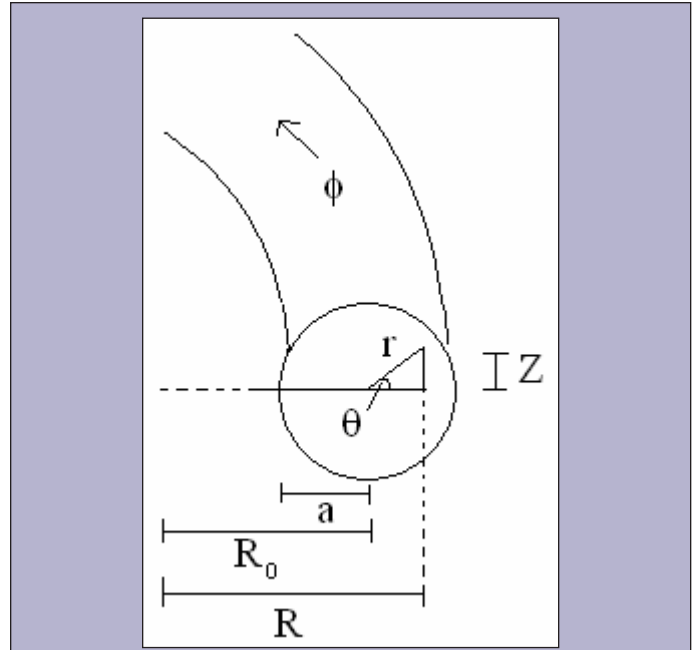


**Figure 1.** Cross-section of plasma showing coordinates and parameters used in analytic derivations.

$$\Psi = \Psi_0 \frac{r^2}{a^2} \quad (5)$$

Here the toroidal radial coordinate  $r$  is related to the cylindrical coordinates  $R, Z$  by:  $R = R_0 + r \cos \theta$ ,  $Z = \kappa r \sin \theta$ , where  $\kappa = Z/(R - R_0)$  is the elongation. Then the magnetic field strength may be written as:

$$B = \sqrt{B_\phi^2 + B_R^2 + B_Z^2} = \sqrt{\frac{B_0^2 R_0^2}{R^2} + \left(-\frac{1}{R} \frac{\partial \Psi}{\partial Z}\right)^2 + \left(\frac{1}{R} \frac{\partial \Psi}{\partial R}\right)^2}$$

$$= \frac{1}{R} \sqrt{B_0^2 R_0^2 + \frac{4\Psi_0^2 r^2}{a^4 \kappa^2} (\sin^2 \theta + \kappa^2 \cos^2 \theta)} \quad (6)$$

The differential of arc length becomes:

$$ds = \sqrt{R^2 d\phi^2 + r^2 d\theta^2}$$

$$= d\theta \sqrt{\frac{B_0^2 R_0^2 a^4 \kappa^2}{4\Psi_0^2 (\sin^2 \theta + \kappa \cos^2 \theta)^2} + r^2 (\sin^2 \theta + \kappa^2 \cos^2 \theta)} \quad (7)$$

The bounce and transit time integral in general cannot be evaluated analytically using these expressions. However, by specializing to low aspect ratio but circular flux surfaces (setting  $\kappa$  to 1), an analytically integrable form arises.

Similarly, by specializing to high aspect ratio but elliptical flux surfaces, an analytically integrable form arises. Taking Taylor expansions of the relevant expressions to first order in the small parameter  $\epsilon = r/R_0 \ll 1$  gives:

$$\frac{1}{\sqrt{E - \mu B}} = \frac{1}{\sqrt{E - \mu B_0}} - \frac{\mu B_0 \cos \theta}{2(E - \mu B_0)^{3/2}} \epsilon + O(\epsilon^2) \quad (8)$$

$$ds \approx \frac{B_0 R_0 a^2 \kappa}{2\Psi_0 (\sin^2 \theta + \kappa \cos^2 \theta)} d\theta \quad (9)$$

Then the bounce and transit times become:

$$\begin{aligned}\tau &= \frac{B_0 R_0 a^2 \kappa}{2\psi_0} \sqrt{\frac{m}{2}} \left[ \frac{1}{\sqrt{E - \mu B_0}} \int \frac{d\theta}{\sin^2 \theta + \kappa \cos^2 \theta} - \frac{\mu B_0 \varepsilon}{2(E - \mu B_0)^{3/2}} \int \frac{\cos \theta}{\sin^2 \theta + \kappa \cos^2 \theta} d\theta + O(\varepsilon^2) \right] \\ &= \frac{B_0 R_0 a^2 \kappa}{2\psi_0} \sqrt{\frac{m}{2}} \left[ \frac{1}{\sqrt{E - \mu B_0}} \frac{\tan^{-1}\left(\frac{\tan \theta}{\sqrt{\kappa}}\right)}{\sqrt{\kappa}} - \frac{\mu B_0 \varepsilon}{2(E - \mu B_0)^{3/2}} \frac{\tanh^{-1}\left(\sin \theta \sqrt{\frac{\kappa-1}{\kappa}}\right)}{\sqrt{\kappa(\kappa-1)}} + O(\varepsilon^2) \right] \\ &\propto \frac{B_0 R_0 a^2 \kappa}{2\psi_0} \sqrt{\frac{m}{2}} \frac{1}{\sqrt{\kappa}} \propto \sqrt{\kappa}\end{aligned}\quad (10)$$

Hence at high aspect ratio the bounce and transit times scale with elongation as  $\sqrt{\kappa}$ .

The Bondeson forms for bounce and transit times scale linearly with the safety factor  $q$ . The scaling of the safety factor with elongation may also be determined. The safety factor is defined as:

$$q = \frac{1}{2\pi} \int_0^{2\pi} \frac{d\varphi}{d\theta} d\theta = \frac{1}{2\pi} \int_0^{2\pi} \frac{r B_\varphi}{R B_\theta} d\theta \quad (11)$$

The toroidal magnetic field  $B_\theta$  may again be taken to vary as  $1/R$ . Then using the expressions above for the components of  $B$  and projecting along the  $\theta$ -direction gives:

$$\begin{aligned}B_\theta &= \frac{2\psi_0}{a^2} \frac{1}{R} \left( \frac{Z \sin \theta}{\kappa^2} + (R - R_0) \cos \theta \right) \\ &= \frac{2\psi_0}{a^2 \kappa} \frac{r}{R} (\sin^2 \theta + \kappa \cos^2 \theta)\end{aligned}\quad (12)$$

Substituting into the expression above for the safety factor gives:

$$\begin{aligned}q &= \frac{1}{2\pi} \int_0^{2\pi} \frac{r B_0 R_0}{R^2} \frac{a^2 \kappa}{2\psi_0} \frac{R}{r} \frac{1}{(\sin^2 \theta + \kappa \cos^2 \theta)} d\theta \\ &= \frac{B_0 a^2 \kappa}{4\pi \psi_0} \int_0^{2\pi} \frac{1}{(1 + \varepsilon \cos \theta)(\sin^2 \theta + \kappa \cos^2 \theta)} d\theta \\ &\propto \frac{B_0 a^2 \kappa}{4\pi \psi_0} \frac{1}{\sqrt{\kappa}} \propto \sqrt{\kappa}\end{aligned}\quad (13)$$

At high aspect ratio the Bondeson forms for bounce and transit times also scale like  $\sqrt{\kappa}$ .

### Numeric Solutions

Numeric solutions for arbitrary aspect ratio and flux surface geometry were also computed using Mathematica and IDL. Numerical singularities were handled by linearizing  $B$  and integrating analytically in the neighborhood of the singularity.

A series of generic plasma equilibria were generated spanning aspect ratios  $A=1.3$  to 10 and elongations  $\kappa=1$  to 2. The equilibria were used to test the numeric solutions in IDL.

Computations were performed in terms of a free parameter  $\gamma$  defined as the ratio of particle parallel velocity  $v_{\parallel}$  to total velocity  $v$ . As  $\gamma$  increases,  $\mu$  decreases, and so the particle becomes less trapped in its orbit. The range of  $\gamma$  values from 0 to 1 captures the full range of variation in  $\mu$ .

The numeric solutions were compared with Bondeson forms using two definitions of the parameter  $\varepsilon$ : first,

$$\varepsilon = \sqrt{\Psi} \frac{a}{R_0} \quad (14)$$

where  $\Psi$  is the normalized poloidal flux, and second,

$$\varepsilon = \frac{B_{\max}(\Psi) - B_{\min}(\Psi)}{B_{\max}(\Psi) + B_{\min}(\Psi)} \quad (15)$$

where  $B_{\max}$  and  $B_{\min}$  are the maximum and minimum values of  $B$  respectively on each flux surface. Similarly, a redefinition of  $R_0$  in the Bondeson forms was also considered:

$$(R_0)_{\text{effective}} = \frac{R_{\max}(\Psi) + R_{\min}(\Psi)}{2} \quad (16)$$

where  $R_{\max}$  and  $R_{\min}$  are the maximum and minimum values of  $R$  respectively on each flux surface.

A simple regression model in the radial coordinate  $r$  and the parameter  $\gamma$  was also applied to transform the Bondeson results into the general geometry solutions for given aspect ratio and elongation.

## RESULTS

Analytic results for bounce and transit times are in Equations 3, 4, and 10 above.

Numeric results are presented in Figures 2-5 below as functions of normalized radial coordinate ( $r/a$ ) for equilibria of varying aspect ratio and elongation. On the left in each figure are plots of numerically-calculated bounce and transit times and corresponding Bondeson forms for four values of the parameter  $\gamma$  described above. The solid lines represent numerically-calculated results and Bondeson results are shown with asterisks. Spikes in the plots occur at the boundary between transit times toward the center of the plasma and bounce times toward the edge. The ratios of the numerically-calculated solutions to the Bondeson forms are plotted on the right in each figure.

Figure 2 shows agreement between numeric solutions and Bondeson forms for high aspect ratio ( $A=10$ ) and circular flux surfaces, using the renormalized definitions

$$\varepsilon = \frac{B_{\max}(\Psi) - B_{\min}(\Psi)}{B_{\max}(\Psi) + B_{\min}(\Psi)} \quad \text{and} \quad (R_0)_{\text{effective}} = \frac{R_{\max}(\Psi) + R_{\min}(\Psi)}{2}.$$

These renormalized expressions for  $\varepsilon$  and  $R_0$  will be used in all further plots and results below.

Figure 3 shows disagreements between numeric solutions and Bondeson forms, for lower aspect ratio ( $A=3$ ) and elliptical flux surfaces ( $\kappa=1.8$ ).

Figure 4 shows pronounced disagreements between numeric solutions and Bondeson forms, for low aspect ratio ( $A=1.3$ ) and elliptical flux surfaces ( $\kappa=2.0$ ).

Figure 5 shows improvements in agreement between numeric solutions and Bondeson forms corrected by simple regression in  $r$  and  $\gamma$ , for low aspect ratio ( $A=1.3$ ) and elliptical flux surfaces ( $\kappa=2.0$ ). On the left are plotted the ratios of the numerically-calculated solutions to the Bondeson forms for four values of  $\gamma$ . On the right

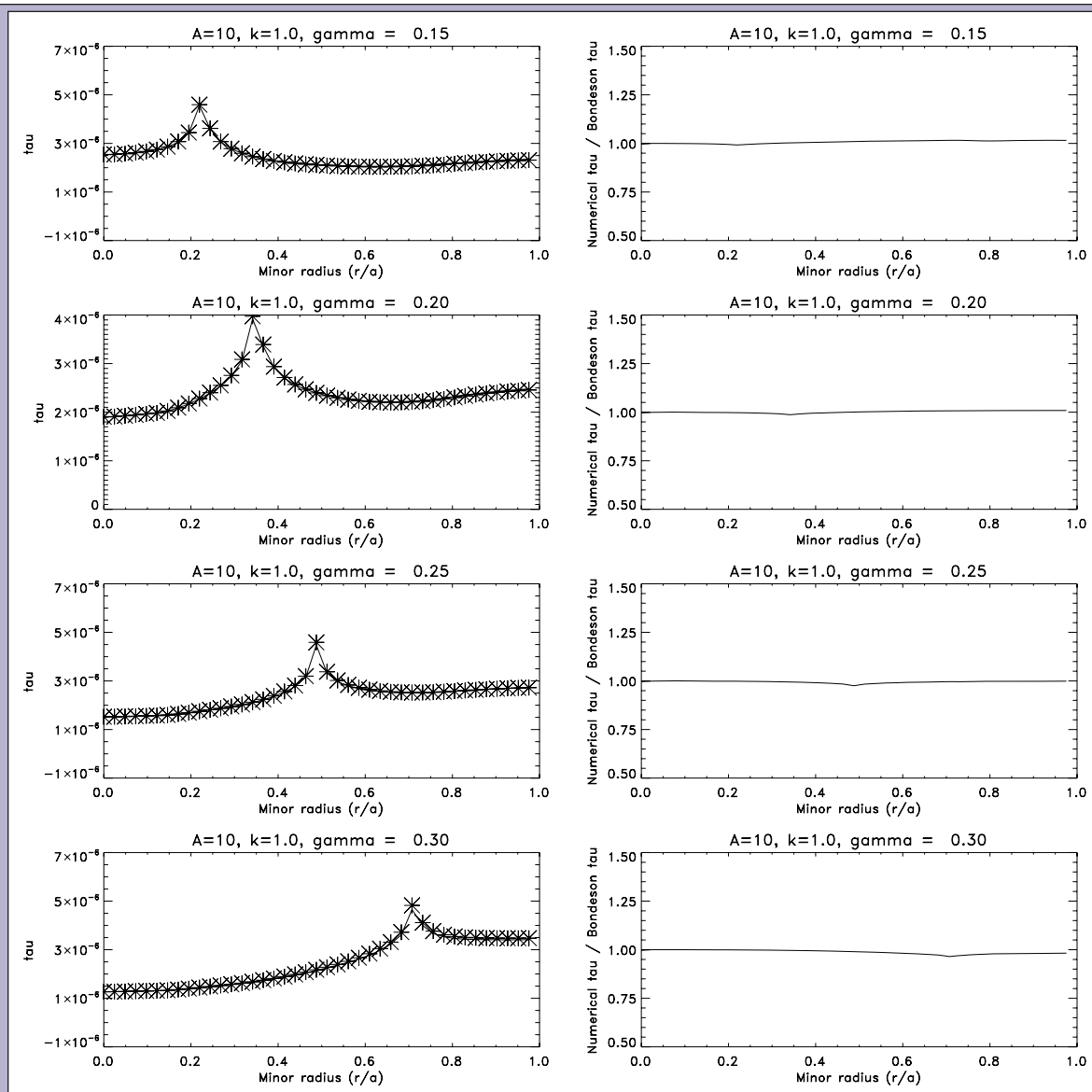


**Figure 2.** Comparison of numeric solutions and Bondeson forms for high aspect ratio ( $A=10$ ) and circular flux surfaces, as functions of normalized minor radius.

are similar plots, but with the Bondeson solutions corrected by simple regression in  $r$  and  $\gamma$ .

## DISCUSSION AND CONCLUSIONS

Analytic solutions for bounce and transit times have been derived as functions of particle energy and magnetic moment for low aspect ratio and elliptical flux surfaces. Numeric solutions for arbitrary aspect ratio and flux surface geometry have also been calculated using Mathematica and IDL and agree with the analytic forms. In typical parameter regimes for the National Spherical Torus Experiment (NSTX), aspect ratios  $A$  around 1.5 and elongations  $\kappa$  around 2 to 3, the deviation between the numeric solutions and the high aspect ratio, circular (Bondeson) approximations can be 40% or more near the edge of the plasma. This result might help assess how accurately kinetic damping theory describes RWM stabilization in NSTX, by experimentally measuring the critical

rotation frequency and comparing it against the value predicted by theory, using generalized orbit times. If theory and experiment are found to agree, generalized orbit times can be used to predict RWM stabilization in low aspect ratio tokamak fusion reactors.

Analytic transformations to map Bondeson solutions into general geometry solutions are currently being investigated. If such transformations can be found, they could be incorporated into stability codes such as MARS to refine predictions of RWM stabilization, with few modifications to the existing code. The regression shown in Figure 5 is a rudimentary attempt at such a transformation. Even using simplistic regression techniques for rescaling, the error in the Bondeson forms could be decreased by as much as 30%.

The aspect ratio dependence of the orbit times was found to be more significant than the elongation dependence. This is likely due to the orbit times scaling with elongation in the same way the safety factor  $q$ , as shown above. Since the Bondeson result is proportional

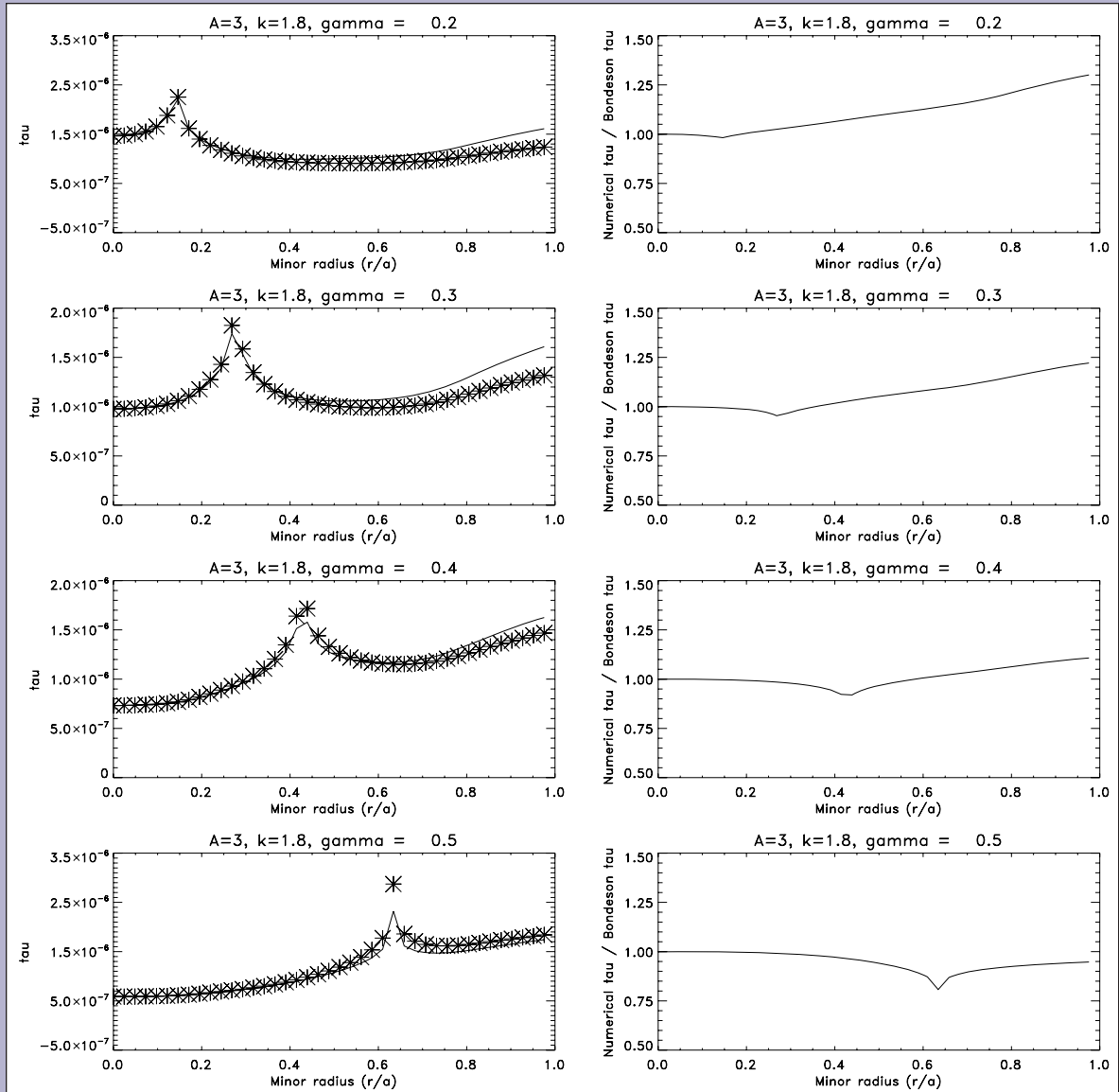


**Figure 3.** Comparison of numeric solutions and Bondeson forms for lower aspect ratio ( $A=3$ ) and elliptical flux surfaces ( $\kappa=1.8$ ), as functions of normalized minor radius..

to  $q$ , it likely captured much of the elongation dependence of the full numeric solution.

For small radial coordinate  $r$  the high aspect ratio approximation  $r/R_0 \ll 1$  should provide reasonable accuracy, and so the numeric solutions and the Bondeson forms should agree. Indeed, for small  $r$  the ratio of numeric solutions to Bondeson solutions was found to be nearly 1 for all values of  $\kappa$  and  $\gamma$ . Hence the Bondeson approximations agree closely with the general geometry solutions in the center of the plasma but deviate from the general solutions at the edge.

Another possibility for future work would be to choose a  $\theta$ -coordinate such that the magnetic field exactly satisfies  $B = B_0(1 - \epsilon \cos \theta)$ , and expand the arc length differential  $ds$  in a Fourier series in this coordinate. Each term of the series would be analytically integrable, and the series might converge quickly to the full numeric solution. This could also be easily incorporated into

stability codes since it would only require elliptic integrals already implemented.

## ACKNOWLEDGMENTS

Thanks to Dr. Jonathan Menard for his time and patience as a mentor, the Science Undergraduate Laboratory Internships program at the U.S. Department of Energy for funding, and Mr. James Morgan for support and administration. This work supported by DOE contract DE-AC02-76CH03073.

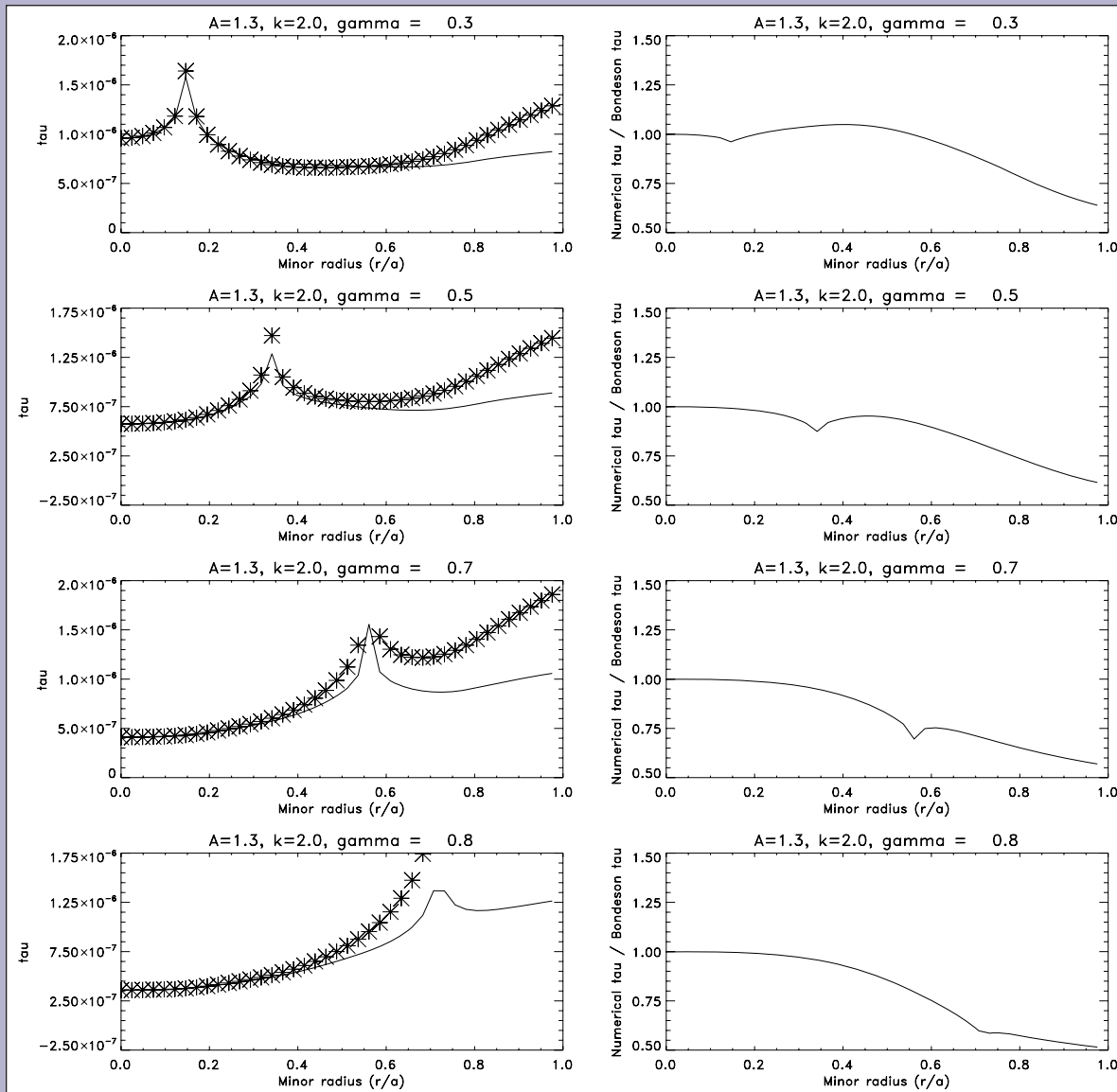


**Figure 4.** Comparison of numeric solutions and Bondeson forms for low aspect ratio ( $A=1.3$ ) and elliptical flux surfaces ( $\kappa=2.0$ ), as functions of normalized minor radius.



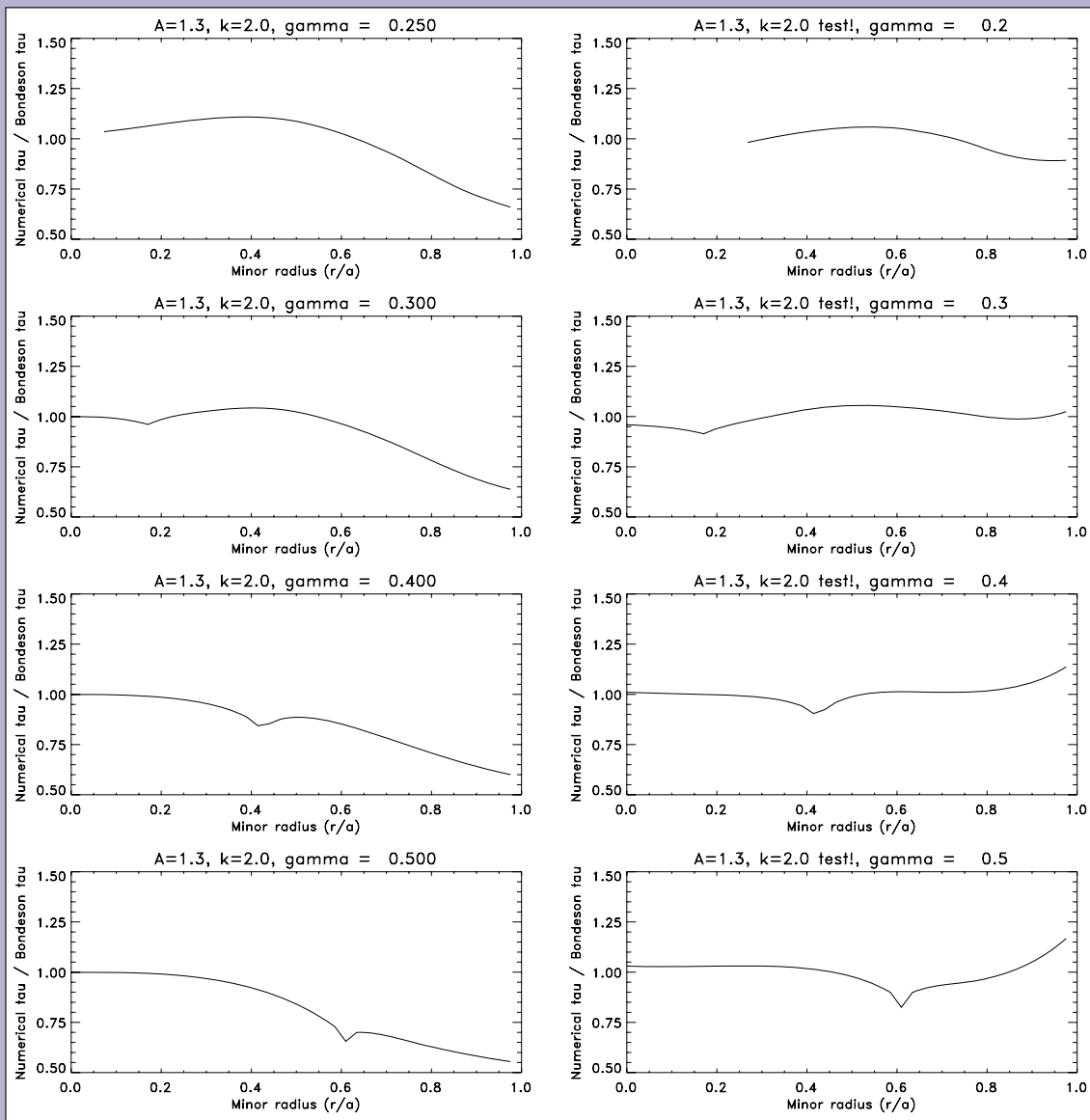


**Figure 5.** Comparison of numeric and Bondeson solutions for low aspect ratio ( $A=1.3$ ) and elliptical flux surfaces ( $\kappa=2.0$ ) with Bondeson solutions transformed by regression in  $r$  and  $\gamma$ .

## REFERENCES

- [1] John Wesson, Tokamaks, Third Edition, Oxford University Press, 2004, pp. 304-342. Wesson's book is an excellent source of background on magnetohydrodynamics and fusion physics in general.
- [2] A. Bondeson and D. J. Ward, "Stabilization of external modes in tokamaks by resistive walls and plasma rotation," in Physical Review Letters, Vol. 72, April 25, 1994, pp. 2709-2712.
- [3] A. M. Garofalo, T. H. Jensen, L. C. Johnson, R. J. La Haye, G. A. Navratil, M. Okabayashi, J. T. Scoville, E. J. Strait, D. R. Baker, J. Bialek, M. S. Chu, J. R. Ferron, J. Jayakumar, L. L. Leo, M. A. Makowski, H. Reimerdes, T. S. Taylor, A. D. Turnbull, M. R. Wade, and S. K. Wong, "Sustained rotational stabilization of DIII-D plasmas above the no-wall beta limit," in Physics of Plasmas, Vol. 9, May 2002, pp. 1997-2005.
- [4] A. Bondeson and M. S. Chu, "Inertia and ion Landau damping of low-frequency magnetohydrodynamical modes in tokamaks," in Physics of Plasmas, Vol. 3, Aug. 1996, pp. 3013-3022.
- [5] R. J. La Haye, A. Bondeson, M. S. Chu, A. M. Garofalo, Y. Q. Liu, G. A. Navratil, M. Okabayashi, H. Reimerdes, and E. J. Strait, "Scaling of the critical plasma rotation for stabilization of the  $n = 1$  resistive wall mode (ideal kink) in the DIII-D tokamak," in Nuclear Fusion, Vol. 44, Nov. 2004, pp. 1197-1203.